



# Tuning catalytic selectivity of liquid-phase hydrogenation of furfural via synergistic effects of supported bimetallic catalysts

Bingfeng Chen, Fengbo Li\*, Zhijun Huang, Guoqing Yuan\*

*Beijing National Laboratory of Molecular Science, Key Laboratory of Green Printing, Institute of Chemistry, Chinese Academy of Sciences, Beijing 100190, PR China*



## ARTICLE INFO

### Article history:

Received 7 January 2015

Received in revised form 28 March 2015

Accepted 9 May 2015

Available online 16 May 2015

### Keywords:

Bimetallic catalysts

Synergistic effect

Hydrogenation

Furfural

Catalytic selectivity

## ABSTRACT

Bimetallic catalysts supported over  $\text{TiO}_2\text{--ZrO}_2$  binary oxides were prepared by co-impregnation methods and used for catalyzing liquid-phase hydrogenation of furfural. Highly selective hydrogenation catalysts can be developed based on bimetallic synergistic effect. The coexistence of small proportion of palladium with supported nickel species greatly improves the catalytic performance and transfer the reaction selectivity from partial hydrogenation to total hydrogenation. The catalyst with Ni-Pd mole ratio of 5:1 shows the best performance. The yield of tetrahydrofurfuryl alcohol (THFA) reaches 93.4%. Ni-Pd synergistic effect is interpreted through XPS measurement and a hydrogen-transfer mechanism is proposed. Pt-Re bimetallic catalyst is an excellent partial hydrogenation catalyst for furfural conversion. Furfural can be totally converted and the selectivity of partial hydrogenation product (FA) reaches 95.7%. When rhenium oxide species are located on the Pt surface, the hydrogen species on Pt are transferred to adsorbed C=O bond to achieve selective hydrogenation.

© 2015 Published by Elsevier B.V.

## 1. Introduction

Limited fossil fuel resources and global warming issues stimulate great research efforts in sustainable production of fuel and chemicals from renewable biomass in recent decades. Furfural from acidic hydrolysis of hemicellulose is the most promising biomass platform chemical that can be manufactured through large-scale industrial process [1]. Through catalytic hydrogenation, furfural can be converted to furfuryl alcohol (FA) and tetrahydrofurfuryl alcohol (THFA). Furfuryl alcohol is widely used to manufacture foundry resins, synthetic fiber, farm chemicals, adhesives and fine chemicals such as vitamin and lysine [2–5]. THFA is considered as a green solvent and used in agricultural applications, printing inks, and industrial and electronics cleaners [6]. Furfural molecule has several active functional groups. There are many possible conversion routes during catalytic hydrogenation, including partial hydrogenation to FA, total hydrogenation to THFA and various possible side reactions such as heat-driven oligomerization, hydrogenolysis of side-substituents to 2-methylfuran, decarbonylation to furan and rearrangement to levulinic acid, and furan ring opening [7]. The core issue of furfural hydrogenation

is how to control its reaction route and hydrogenation degree through using highly selective catalyst.

The performance of heterogeneous hydrogenation catalysts is directly related to active metals and supports [8]. Supported noble and non-noble metals have been reported for hydrogenation of FR. Conventional production of THFA is based on a two-step strategy: hydrogenation of furfural FA over Cu-Cr catalyst and further hydrogenation of FA to THFA over supported noble catalysts. Direct hydrogenation of furfural to THFA has been achieved over Ni-Pd/SiO<sub>2</sub> [9], Ni/SiO<sub>2</sub> [10] and Pd/MFI [11] catalysts. The catalysts for hydrogenation of furfural to FA are supported Ni, Co, Cu, Ru, Pd and their bimetallic catalysts [2,12,13]. Pt-based catalysts are rarely used for producing FA from furfural due to complex side reactions (hydrogenolysis of the C=O bond, decarbonylation, total hydrogenation and furan ring opening, etc.) [14]. It has not been reported that the hydrogenation degree can be adjusted through synergistic effects of bimetallic catalytic system. It is of great significant to achieve both selective hydrogenation and total hydrogenation of furfural through a well-defined bimetallic mechanism.

Physicochemical properties of the catalyst's support markedly influence its performance for liquid-phase catalytic hydrogenation of unsaturated aldehydes and ketones [8].  $\text{TiO}_2\text{--ZrO}_2$  mixed oxides exhibit high surface area, profound surface acid-base properties, a high thermal stability, and strong mechanical strength [15].  $\text{TiO}_2\text{--ZrO}_2$  mixed oxides are used as catalysts and catalysts supports for various reactions [16].  $\text{TiO}_2\text{--ZrO}_2$  supported Pt species are

\* Corresponding authors. Tel.: +86 10 62634920; fax: +86 10 62559373.

E-mail addresses: [lifb@iccas.ac.cn](mailto:lifb@iccas.ac.cn) (F. Li), [yuangq@iccas.ac.cn](mailto:yuangq@iccas.ac.cn) (G. Yuan).

the most selected catalysts for hydrogenation conversion such as naphthalene hydrogenation [17], selective hydrogenation of furfural [12], and selective hydrogenation of crotonaldehyde [18].  $\text{TiO}_2\text{-ZrO}_2$  mixed oxides are used as supports of bimetallic catalysts for selective furfural hydrogenation.

In this work, Ni-Pd over  $\text{TiO}_2\text{-ZrO}_2$  was selected as model catalytic system to investigated synergistic effects of bimetallic catalysts upon selectivity of liquid-phase furfural hydrogenation. Raney Ni and Pd/C were used as benchmarked catalysts. The bimetallic catalysts with various ratio of Ni to Pd were screened and the experimental results showed marked synergistic effects. The corresponding mechanism was revealed by XPS measurement. In further investigation, the selectivity of Pt-M/ $\text{TiO}_2\text{-ZrO}_2$  bimetal catalysts ( $M = \text{Re}, \text{Sn}, \text{In}$ ) for furfural hydrogenation was explored and a different trend of bimetallic synergistic effect was observed.

## 2. Experiment

### 2.1. Materials and chemicals

Titanium butoxide, Zirconium (IV) butoxide solution (80 wt% in n-butanol), dodecyl amine (DDA), nickel nitrate hexahydrate, furfural, ethanol, toluene, dioxane, and 2-propanol were purchased from Sinopharm Chemical Reagent.  $\text{H}_2\text{PtCl}_6$ ,  $\text{KReO}_4$ ,  $\text{PdCl}_2$ , Pd/C and Raney Ni were purchased from Strem.  $\text{SnCl}_4\cdot 5\text{H}_2\text{O}$  and  $\text{In}(\text{SO}_3\text{CF}_3)_3$  were obtained from Alfa Aesar. All the reagents were used as received except furfural, which was used after vacuum distillation.

### 2.2. Catalyst preparation

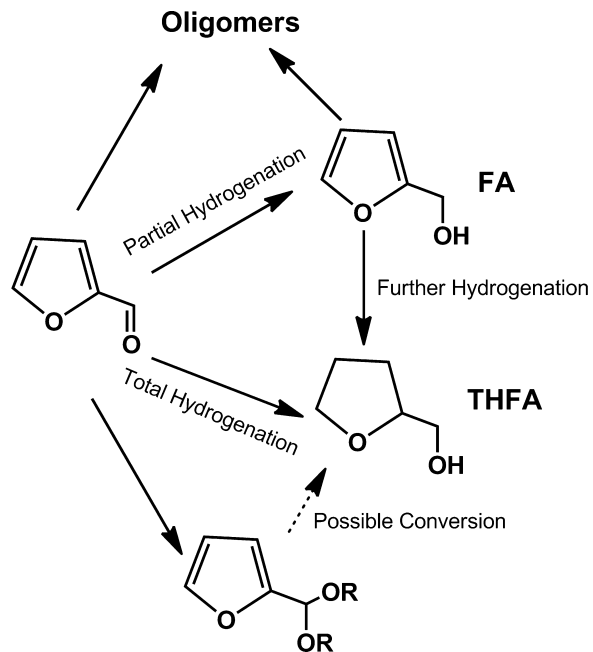
$\text{TiO}_2\text{-ZrO}_2$  mixed oxide support (1:1, mole ratio) was prepared by the sol-gel method reported by our group [19]. All catalysts were prepared by co-impregnation or impregnation of metal precursors onto  $\text{TiO}_2\text{-ZrO}_2$  binary oxide support. The calculated amount of  $\text{TiO}_2\text{-ZrO}_2$  was impregnated with a certain concentration aqueous solution of metal precursors (such as  $\text{PdCl}_2(\text{CH}_3\text{CN})_2$ ,  $\text{Ni}(\text{NO}_3)_2\cdot 6\text{H}_2\text{O}$ ,  $\text{H}_2\text{PtCl}_6$ ,  $\text{KReO}_4$ ,  $\text{SnCl}_4\cdot 5\text{H}_2\text{O}$  and  $\text{In}(\text{SO}_3\text{CF}_3)_3$ ) and kept in an oven at 383 K overnight. Then these solids were calcined at 723 K in air for 3 h. These catalysts were activated under flowing diluted hydrogen ( $\text{H}_2/\text{Ar}: 10\%$ ) at 673 K for 3 h before testing.

### 2.3. Catalytic activity measurements

Catalytic hydrogenation of furfural was performed in a 100 ml stainless autoclave equipped with a pressure gauge, a magnetic stirrer, and an electric temperature controller. The catalyst (200.0 mg), the solvent (8.5 ml) and furfural (1.5 ml) were introduced into the reactor. The sealed autoclave was flushed with  $\text{H}_2$  three times, pressurized with  $\text{H}_2$  to 5.0 MPa, and started to stir. After the designated temperature was reached, the reaction began. At the end of reaction, the autoclave was cooled to ambient temperature and slowly depressurized. The conversion and product composition were analyzed by GC and GC-MS. GC was performed on a GC-2014 (SHIMADZU) equipped with a high-temperature capillary column (MXT-1, 30 m, 0.25 mm ID) and a FID detector. GC-MS was performed on a GCT Premier/Waters instrument equipped with a capillary column (DB-5MS/J&W Scientific, 30 m, 0.25 mm ID).

### 2.4. Catalyst characterization

Powder X-ray diffraction (XRD) patterns was measured on a Rigaku Rotaflex diffractometer equipped with a rotating anode and a Cu-K $\alpha$  radiation source (40 kV, 200 MA;  $\lambda = 1.54056\text{\AA}$ ). XPS data were obtained with an ESCALab220i-XL electron spectrometer from VG Scientific using 300 W Al-K $\alpha$  radiations. The base pressure was approximately  $3 \times 10^{-9}$  mbar. The binding energies



Scheme 1. Illustration of reaction routes of furfural hydrogenation.

were referenced to the C1s line at 284.8 eV from adventitious carbon. The Eclipse V2.1 data analysis software supplied by the VG ESCA-Lab200I-XL instrument manufacturer was used to manipulate the acquired spectra. Transmission electron microscopy (TEM) was performed on a JEOL 2010 TEM equipped with an attachment for local energy dispersion analysis (EDX). The accelerating voltage was 200 kV, and the spot size was 1.0 nm.

## 3. Results and discussions

### 3.1. Hydrogenation of furfural over Ni-Pd bimetallic catalysts

Scheme 1 shows reaction route map of liquid-phase hydrogenation of furfural in alcohol solvents. There are two target molecules: partial hydrogenation product (FA) and total hydrogenation product (THFA). Cu-Cr mixed oxides are the classic catalysts for partial hydrogenation of furfural. However, leached toxic Cr species pose serious environmental issues. Nickel-based catalysts are considered as potential replacement. The main drawback of nickel hydrogenation catalyst is that active zero-valent nickel species are highly sensitive to oxygen. It is difficult to keep nickel catalysts in their primary activated states. Fresh commercial Raney Ni shows low catalytic activity and poor selectivity of FA (Entry 1 in Table 1). Nickel over  $\text{TiO}_2\text{-ZrO}_2$  binary oxide has improved catalytic activity for partial hydrogenation of furfural and the yield of FA reaches 69.2% (Entry 2 in Table 1). The reaction over the supported Pd catalyst mainly produces total hydrogenation product. The yield of THFA is 62.2% for furfural hydrogenation over commercial Pd/C and the value increases to 78.6% for palladium over  $\text{TiO}_2\text{-ZrO}_2$  binary oxide (Entry 3, 4 in Table 1).

When nickel and palladium precursors are introduced onto  $\text{TiO}_2\text{-ZrO}_2$  through co-impregnation, Ni-Pd/ $\text{TiO}_2\text{-ZrO}_2$  bimetallic catalyst is obtained. The coexistence of nickel and palladium lead to marked synergistic effects and enhance the catalytic performance significantly (Entry 5–8 in Table 1). Ni-Pd bimetallic catalysts show higher hydrogenation activity than anyone of the two mono-metallic catalysts. The yield values of hydrogenation products are above 90% and the percentage of byproducts is very low. Though adjusting the mole ratio of nickel to palladium, the catalytic selectivity is finely tuned to only one type of hydrogenation

**Table 1**

Screening experimental results of furfural hydrogenation over supported nickel and palladium catalysts.

Entry	Catalysts	Hydrogenation product yield (%)		Others (%) <sup>c</sup>
		FA	THFA	
1	Raney Ni <sup>a</sup>	29.0	8.3	23.3
2	Ni/TiO <sub>2</sub> –ZrO <sub>2</sub> (5.0 wt%)	69.2	26.4	3.13
3	Pd/C (5.0 wt%)	14.1	62.2	11.5
4	Pd/TiO <sub>2</sub> –ZrO <sub>2</sub> (5.0 wt%)	3.8	78.6	16.1
5	Ni–Pd (7:1) <sup>b</sup>	39.1	59.8	1.1
6	Ni–Pd (5:1)	2.1	93.4	3.9
7	Ni–Pd (3:1)	3.3	86.4	10.3
8	Ni–Pd (1:1)	1.6	84.1	9.7

<sup>a</sup> Raney Ni (11.2 mg; ca. 0.17 mmol Ni).

<sup>b</sup> Ni–Pd/TiO<sub>2</sub>–ZrO<sub>2</sub> (Ni load: 5 wt%, 0.2 g; 0.17 mmol Ni), the value in brackets is mole ratio of nickel to palladium.

<sup>c</sup> Acetals and oligomers.

Reaction conditions: furfural (1.5 ml), ethanol (8.5 ml), catalysts (0.2 g), pressure of hydrogen (5.0 MPa), reaction temperature: 403 K, reaction time: 8 h. FA: furfuryl alcohol; THFA: tetrahydrofurfuryl alcohol.

product. Addition of small proportion of palladium directly transfers the catalytic performance of supported nickel from partial hydrogenation catalyst to total hydrogenation catalyst. The bimetallic catalyst with Ni–Pd mole ratio of 5:1 shows the best performance. The yield of THFA reaches 93.4% and the percentage of useless byproducts is only 3.9%. These findings have the practical significance that supported nickel species can be transformed into highly active hydrogenation catalysts through being doped with a small proportion of palladium and the resulting catalysts even show higher activity than the supported palladium catalysts with the same metal load. The increase of palladium load of Ni–Pd bimetallic catalyst leads to gradual decrease of THFA yield.

Ni–Pd (5:1)/TiO<sub>2</sub>–ZrO<sub>2</sub> is a highly active hydrogenation catalyst. After the reaction runs for 1.5 h, 97.3% conversion of furfural is achieved and the hydrogenation products include FA (39.8%) and THFA (38.4%) (Fig. 1a). FA is further hydrogenated to THFA. Solvent effect also influences catalytic activity and selectivity of liquid-phase hydrogenation of furfural [20,21]. Fig. 1b shows experimental results of furfural hydrogenation in various solvent. The reaction is carried out over Ni–Pd/TiO<sub>2</sub>–ZrO<sub>2</sub> (Ni/Pd = 5) at 403 K and under 5 MPa of H<sub>2</sub>. The selected solvents include ethanol, 2-propanol, 1,4-dioxane, and toluene. The selectivity of THFA shows the following sequence: ethanol > 1,4-dioxane > 2-propanol > toluene. This trend is roughly consistent with the order of solvent polarity:  $E_N^T$ (ethanol, 0.654) >  $E_N^T$ (2-propanol, 0.546) >  $E_N^T$  > (1,4-dioxane, 0.164) >  $E_N^T$ (toluene, 0.099) ( $E_N^T$  solubility parameter of the solvent polarity) [22]. When alcohols are used as solvents for aldehyde hydrogenation, acetals are typical byproducts [23]. As confirmed by GC-MS, 2-furaldehyde diisopropyl acetal and 2-furaldehyde diethyl acetal are detected after furfural is hydrogenated in 2-propanol and ethanol. TiO<sub>2</sub>–ZrO<sub>2</sub> binary oxides have surface acidity by charge imbalance of Ti–O–Zr bonding [24,25]. TiO<sub>2</sub>–ZrO<sub>2</sub> with equal proportion of Ti and Zr shows the highest surface acid strength [16]. Acetalization is correlated with surface acid of catalyst support. This side reaction has also been reported for liquid hydrogenation of furfural using Ir/Nb<sub>2</sub>O<sub>5</sub> in alcohol [26]. The formation of hemiacetal byproducts has been reported for Ir/TiO<sub>2</sub>-catalyzed furfural hydrogenation in ethanol [27].

TiO<sub>2</sub>–ZrO<sub>2</sub> mixed oxides not only have the advantages of both TiO<sub>2</sub> as active catalyst or support and ZrO<sub>2</sub> as acid-base sites, but also exhibit novel catalytic properties imparted by the formation of active intermediate states. TiO<sub>2</sub>–ZrO<sub>2</sub> mixed oxide (Ti/Zr, 1:1) is calcined at 823 K and the crystalline ZrTiO<sub>4</sub> is formed. The materials are mixtures of ZrTiO<sub>4</sub> nanocrystals and amorphous mixed oxides. The size of ZrTiO<sub>4</sub> nanocrystals is in the range from 5 nm to 10 nm,

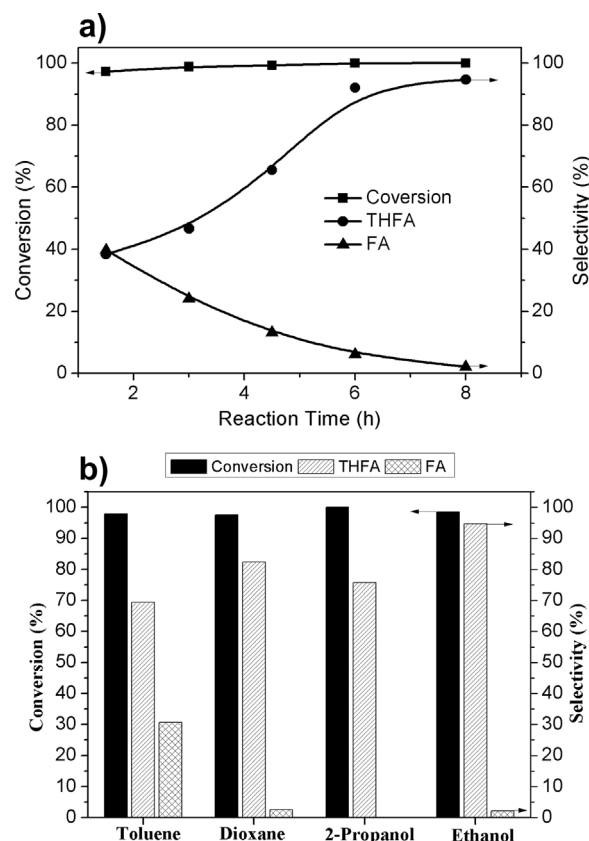
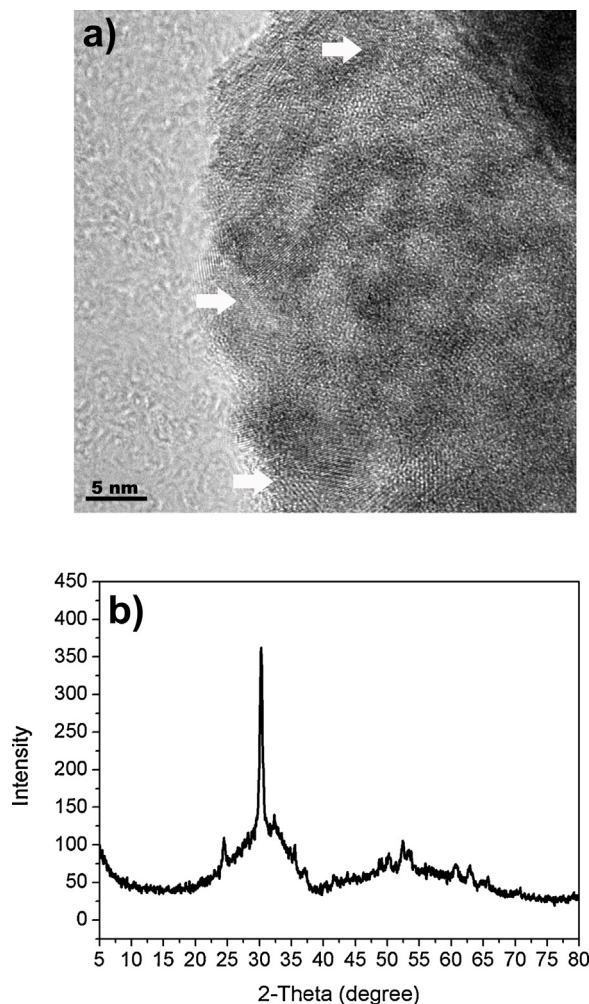


Fig. 1. (a) Reaction curves on time of furfural hydrogenation over Ni–Pd (5:1)/TiO<sub>2</sub>–ZrO<sub>2</sub> catalyst. (b) Experimental results of furfural hydrogenation over Ni–Pd (5:1)/TiO<sub>2</sub>–ZrO<sub>2</sub> catalyst in various solvents.

which are embedded in the mixed oxide matrix and give novel catalytic properties of TiO<sub>2</sub>–ZrO<sub>2</sub> binary oxide (Fig. 2). The amorphous TiO<sub>2</sub>–ZrO<sub>2</sub> mixed oxide (Ti/Zr, 1:1) has a high surface area of 243 m<sup>2</sup>/g and the average pore size is 1.66 nm [19]. Fig. 3a shows TEM image of porous structures of Ni–Pd (5:1)/TiO<sub>2</sub>–ZrO<sub>2</sub> bimetal catalyst. Energy-dispersive X-ray analysis (EDX) was employed to confirm the existence of nickel and palladium species over the support. EDX spectrum of Ni–Pd/TiO<sub>2</sub>–ZrO<sub>2</sub> (Fig. 3b) shows peaks of Ni, Pd, Ti, Zr, O and Cu. The signals of copper are from supporting grid for TEM sample preparation.

### 3.2. Tuning selectivity via synergistic effects of supporting Ni–Pd bimetallic catalysts

The results in Table 1 reveal marked synergistic effects between nickel and palladium for catalytic liquid-phase hydrogenation of furfural. A highly active and selective catalyst can be developed through doping supported nickel with palladium of one fifth of nickel load. Ni–Pd synergistic effect has been found in catalytic hydrogenation of nitrobenzene over Ni–Pd bimetallic catalyst supported by Ti containing mesoporous silica. The optimal molar ratio of nickel to palladium is 1.5 [28]. EDX spectrum has demonstrated the coexistence of nickel and palladium over TiO<sub>2</sub>–ZrO<sub>2</sub>. However, there is no detailed information about the chemical states of nickel species and palladium species. To reveal the mechanism of Ni–Pd bimetallic synergistic effect, XPS measurement is performed to exam the chemical states of supported nickel species and palladium species. Fig. 4a shows the XPS survey spectrum of Ni–Pd (5:1)/TiO<sub>2</sub>–ZrO<sub>2</sub> bimetallic catalyst. Typical elements are detected. The metal load of palladium is relatively low and Pd 3d XPS peaks are overlapped with strong Zr 3p peaks. These make Pd 3d XPS



**Fig. 2.** (a) TEM image of ZrTiO<sub>4</sub> microcrystals embedded in TiO<sub>2</sub>-ZrO<sub>2</sub> (1:1; 823 K) mixed oxide matrix. (b) Powder XRD pattern of TiO<sub>2</sub>-ZrO<sub>2</sub> (1:1; 823 K) mixed oxide.

peaks hardly suitable for interpreting Ni-Pd synergistic effect. Fitting of the XPS envelope of Zr 3p results in identification of Pd 3d peaks (Fig. 4b). However, the overlap with strong Zr 3p signals makes binding energy measurement not quite accurate.

Ni 2p XPS peaks have complicated patterns, but more useful chemical information about the synergistic effect. XPS measurement and calculation are performed over four selected model samples: Ni/TiO<sub>2</sub>-ZrO<sub>2</sub> (A, reduced by hydrogen flow and stored in argon), Ni/TiO<sub>2</sub>-ZrO<sub>2</sub> (B, separated A after one-batch hydrogenation, dried and stored in pure hydrogen), Ni-Pd (5:1)/TiO<sub>2</sub>-ZrO<sub>2</sub> (C, reduced by hydrogen flow and stored in argon), and Ni-Pd (5:1)/TiO<sub>2</sub>-ZrO<sub>2</sub> (D, separated C after one-batch hydrogenation, dried and stored in pure hydrogen) (Fig. 5). Fitting of Ni 2p XPS envelope results in identification of two chemical states of nickel species and their satellite peaks. Ni 2p<sub>3/2</sub> at binding energy of 851.4 eV and Ni 2p<sub>1/2</sub> (851.4 + 17.3 eV) are attributed to zero-valent nickel species. Ni 2p<sub>3/2</sub> standard value of bulk nickel is 852.6 eV [29]. Nickel species supported over TiO<sub>2</sub>-ZrO<sub>2</sub> show a little shift (1.2 eV) in their Ni 2p<sub>3/2</sub> binding energies (BE) from the standard value. This may be attributed to the strong interaction between nickel species and TiO<sub>2</sub>-ZrO<sub>2</sub> support [30]. Ni 2p<sub>3/2</sub> at binding energy of 854.9 eV and Ni 2p<sub>1/2</sub> (854.9 + 18.3 eV) are indexed to electro-deficient nickel species (Ni<sup>2+</sup>) [31]. There are some broad bands following Ni 2p<sub>3/2</sub> and Ni 2p<sub>1/2</sub> that are caused by satellite peaks. After being activated by hydrogen at relatively high temperature, the proportion of active zero-valent nickel species is very low

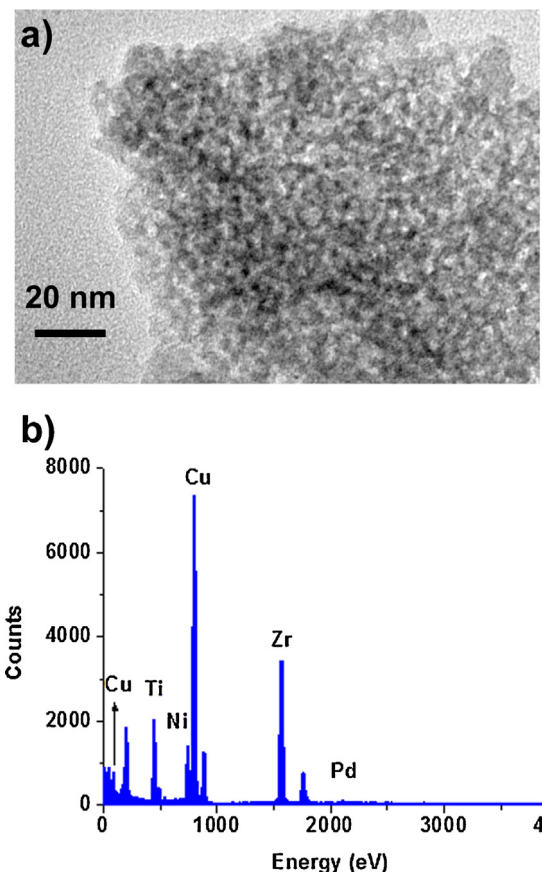


**Fig. 3.** (a) TEM image of Ni-Pd (5:1)/TiO<sub>2</sub>-ZrO<sub>2</sub>. (b) EDX spectrum of the selected sample of Ni-Pd (5:1)/TiO<sub>2</sub>-ZrO<sub>2</sub>.

for Ni/TiO<sub>2</sub>-ZrO<sub>2</sub> (A in Fig. 5). The proportion has small variation during catalytic hydrogenation process (B in Fig. 5). This results in its low catalytic activity for furfural hydrogenation. For Ni-Pd (5:1)/TiO<sub>2</sub>-ZrO<sub>2</sub>, the proportion of active zero-valent nickel species has a marked increase (approximately 20.2%) (C in Fig. 5). The addition of Pd increases the reducibility of supported nickel species and similar phenomenon has been observed for Ni-Pd/Al<sub>2</sub>O<sub>3</sub> bimetallic catalyst [32]. It is noteworthy that the coexistence of nickel and palladium makes supported nickel species highly dynamic during hydrogenation process. The proportion of zero-valent nickel species sharply increases to 42.9% after one-run furfural hydrogenation testing of Ni-Pd (5:1)/TiO<sub>2</sub>-ZrO<sub>2</sub> (D in Fig. 5). Active zero-valent nickel species are *in situ* formed during hydrogenation process. This directly leads to greatly improved catalytic performance. The presence of palladium is the crucial factor *in situ* forming zero-valent nickel species. A hydrogen-transfer mechanism is proposed to interpret Ni-Pd synergistic effect (Scheme 2). Supported nickel species and palladium species should achieve a well-doped dispersion state. Palladium nanoparticles are kept in small size and uniformly embedded with nickel species. Molecular hydrogen is adsorbed and activated by palladium species and adjacent nickel species are facilely reduced to active zero-valent sites. This conversion significantly increases the surface concentration of catalytic active sites for furfural hydrogenation. However, such positive synergistic effect of Ni-Pd might be spoilt by loss of the required doping dispersion state. As revealed by experimental results (Table 1), the addition of palladium metal load has a negative effect upon the catalytic performance. Further increase of palladium proportion from 20% to 50% makes the catalytic performance more like monometallic palladium catalyst.

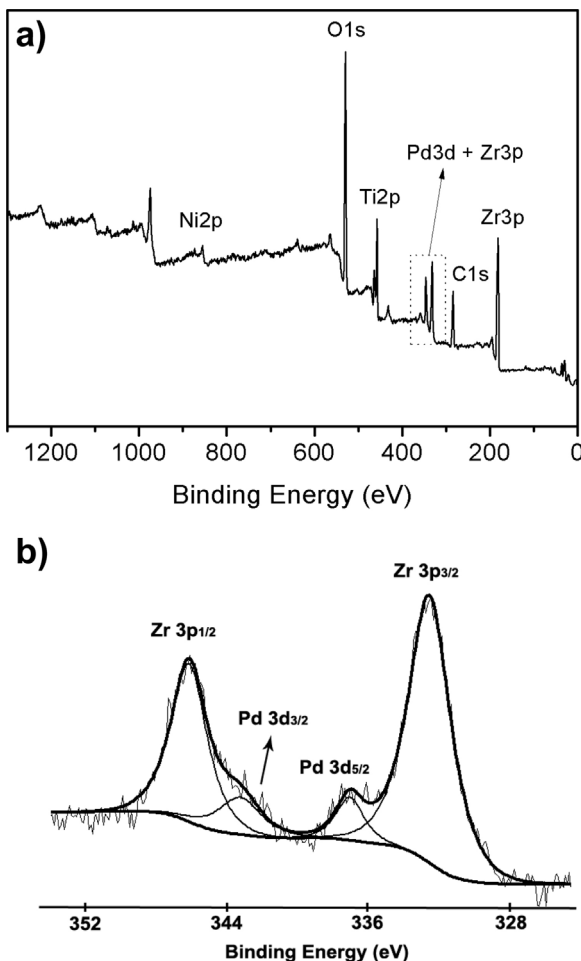


**Fig. 4.** (a) XPS survey spectrum of Ni-Pd (5:1)/TiO<sub>2</sub>-ZrO<sub>2</sub>. (b) Fitting of XPS envelopes of Zr 2p and Pd 3d.

### 3.3. Catalytic selectivity of furfural hydrogenation over Pt-M bimetallic catalysts (M: Re, In, Sn)

Table 2 lists experimental results of furfural hydrogenation over TiO<sub>2</sub>-ZrO<sub>2</sub> supported Pt-M bimetallic catalysts. The hydrogenation over Pt/TiO<sub>2</sub>-ZrO<sub>2</sub> leads to 49.6% of furfural conversion and product mixtures of FA (5.6%), THFA (49.6%), and ring-opening products (44.8%). Ring-opening products, including ethyl levulinate ester and 5,5-diethoxypentan-2-one, are produced through hydrogenation of furfural and the following alcoholysis of furfuryl alcohol. These products can be explained by the bifunctional catalyst Pt/TiO<sub>2</sub>-ZrO<sub>2</sub>: hydrogenation activity and acidity of support. Similar results have been observed by our group using the

**Table 2**

Experimental results of TiO<sub>2</sub>-ZrO<sub>2</sub> supported Pt-M (M: Re, In, Sn) catalysts in selective hydrogenation of furfural.

TiO <sub>2</sub> -ZrO <sub>2</sub> supported catalysts	FR conv. (%)	Selectivity (%)		
	FA	THFA	Acetal	Others
Pt (2 wt.%)	49.6	5.6	49.6	—
Re (1 wt.%)	44.6	57.6	—	29.1
Pt (2 wt.%)–Re (1 wt.%)	100	95.7	1.3	3.0
Pt (2 wt.%)–In (2 wt.%)	73.3	74.9	7.1	14.5
Pt (2 wt.%)–Sn (2 wt.%)	98.3	47.8	35.4	1.7
				15.1

Reaction conditions: catalyst (0.2 g), furfural (1.5 ml), ethanol (8.5 ml), H<sub>2</sub> (5.0 MPa); reaction temperature: 403 K, reaction time: 8 h. FR: furfural; FA: furfuryl alcohol; THFA: Tetrahydrofurfuryl alcohol; Acetal: 2-(diethoxymethyl)furan.

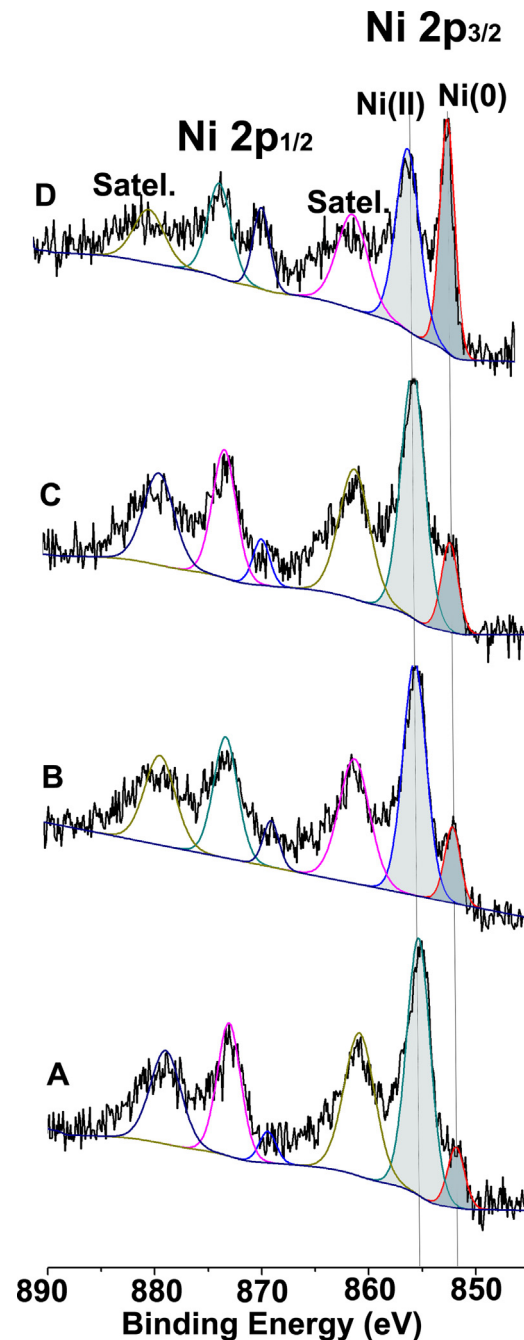
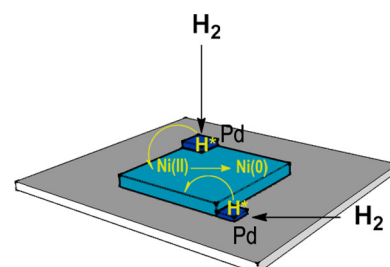


**Fig. 5.** Fitting of Ni 2p XPS envelopes of four selected model samples: Ni/TiO<sub>2</sub>-ZrO<sub>2</sub> (A, reduced by hydrogen flow and stored in argon), Ni/TiO<sub>2</sub>-ZrO<sub>2</sub> (B, separated A after one-batch hydrogenation, dried and stored in pure hydrogen), Ni-Pd (5:1)/TiO<sub>2</sub>-ZrO<sub>2</sub> (C, reduced by hydrogen flow and stored in argon), and Ni-Pd (5:1)/TiO<sub>2</sub>-ZrO<sub>2</sub> (D, separated C after one-batch hydrogenation, dried and stored in pure hydrogen).



**Scheme 2.** Proposed mechanism of nickel–palladium synergistic effect.

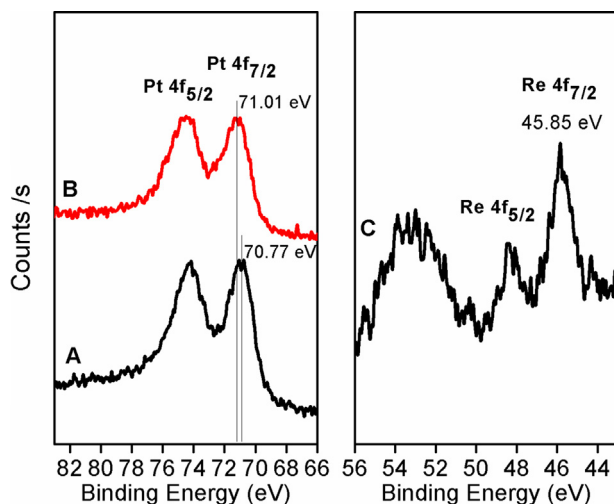


**Fig. 6.** Pt 4f XPS peaks of Pt (2 wt%)/TiO<sub>2</sub>-ZrO<sub>2</sub> (A) and Pt (2 wt%)-Re (1 wt%)/TiO<sub>2</sub>-ZrO<sub>2</sub> (B); Re 4f XPS peaks of Pt (2 wt%)-Re (1 wt%)/TiO<sub>2</sub>-ZrO<sub>2</sub> (C).

bifunctional catalyst Pt/ZrNbPO<sub>4</sub> in the conversion of furfural [33]. The low selectivity has also been reported for furfural hydrogenation over Pt/C [2] and Pt/Al<sub>2</sub>O<sub>3</sub> catalysts [12]. The main products of furfural hydrogenation over Re/TiO<sub>2</sub>-ZrO<sub>2</sub> are FA (57.6%) and acetal of furfural (29.1%). Pt-Re bimetallic catalyst shows excellent catalytic activity and selectivity. Furfural is totally converted and the selectivity of partial hydrogenation product (FA) reaches 95.7%. In and Sn are introduced as the second metal and show positive effects upon catalytic activity. Pt-Sn bimetallic catalyst has high furfural conversion (98.3%), but the selectivity is relatively poor. Pt-In bimetallic catalyst can convert 73.3% of furfural and the selectivity of FA is 74.9%.

Ni-Pd bimetallic catalyst is highly active for total hydrogenation of furfural and Pt-Re bimetallic catalyst especially converts furfural into partial hydrogenation product (FA). Chemical states of Pt-Re/TiO<sub>2</sub>-ZrO<sub>2</sub> catalyst are measured by XPS (Fig. 6). Pt 4f<sub>7/2</sub> XPS peak of Pt/TiO<sub>2</sub>-ZrO<sub>2</sub> is at the binding energy of 70.77 eV and the value measured over Pt-Re/TiO<sub>2</sub>-ZrO<sub>2</sub> is 71.01 eV (Fig. 6A and B). The tiny difference may be attributed to measurement error. Supported platinum species of Pt/TiO<sub>2</sub>-ZrO<sub>2</sub> and Pt-Re/TiO<sub>2</sub>-ZrO<sub>2</sub> are kept in zero-valent state. Re 4f<sub>7/2</sub> peak is detected at the binding energy of 45.85 eV, which is indexed to middle chemical states between Re<sup>6+</sup> and Re<sup>7+</sup>. It has been reported that Re 4f<sub>7/2</sub> of ReO<sub>3</sub> is at the BE of 45.2 eV [34] and Re 4f<sub>7/2</sub> of Re<sub>2</sub>O<sub>7</sub> is at the BE of 46.4 eV [35]. This finding implies that Re<sub>2</sub>O<sub>7</sub> or ReO<sub>3</sub> may be *in situ* converted to catalytic active species for hydrogenation of furfural. Similar results have been observed by Pascoe and Broadbent that cinnamaldehyde and crotonaldehyde have been hydrogenated to cinnamyl alcohol and crotyl alcohol by Re<sub>2</sub>O<sub>7</sub> catalysts [36,37]. The side-reaction of acetalization is correlated with surface acid of the catalyst support. This phenomenon has been reported over other catalysts in catalytic hydrogenation of furfural [38].

In this work, the synthesized TiO<sub>2</sub>-ZrO<sub>2</sub> composite oxide was selected as catalyst support. Both TiO<sub>2</sub> and ZrO<sub>2</sub> have been used as reducible supports in chemoselective hydrogenation and known as strong metal-support interactions (SMSI) properties [8]. During activation of catalysts, TiO<sub>2</sub> was reduced into the lower valence of titanium (Ti<sup>3+</sup>), and the reduced support transformed part of electrons to the active metal Pt particle. This interaction has been confirmed by the fact that Pt 4f<sub>7/2</sub> of Pt/TiO<sub>2</sub>-ZrO<sub>2</sub> is at the binding energy of 70.77 eV, which is lower than that of Pt foil (71.4 eV). Similar results have been reported by Peter Claus that gold is negatively charged in Au/TiO<sub>2</sub> catalyst [39]. The presence of oxidized state of second metals such as rhenium oxide is helpful to activate the C=O

bond [40]. When metal oxide species are located on the Pt surface, the hydrogen species on Pt are transferred to adsorbed C=O bond to achieve selective hydrogenation. Pt-Re catalyst exhibits the best performance with yield of furfuryl alcohol 95.7%.

#### 4. Conclusions

In summary, a strategy based on bimetallic synergistic effect was developed to tune the catalytic selectivity of liquid-phase furfural hydrogenation. TiO<sub>2</sub>-ZrO<sub>2</sub> binary oxide was synthesized as the support for monometallic or bimetallic catalyst. Addition of small proportion of palladium directly transfers the catalytic performance of supported nickel from partial hydrogenation catalyst to total hydrogenation catalyst. The bimetallic catalyst with Ni-Pd mole ratio of 5:1 shows the best performance. The yield of THFA reaches 93.4% and the percentage of useless byproducts is only 3.9%. Ni-Pd synergistic effect was interpreted through the hydrogen-transfer mechanism, which significantly increases the surface concentration of catalytic active sites for furfural hydrogenation. Pt-Re bimetallic catalyst especially converts furfural into partial hydrogenation product (FA). Furfural is totally converted and the selectivity of partial hydrogenation product (FA) reaches 95.7%. This excellent performance is achieved through synergistic effect of supported rhenium oxide species and platinum species.

#### Acknowledgement

This work was financially supported by the National Natural Sciences Foundation of China (nos. 21174148, 21403248, 21304101).

#### Appendix A. Supplementary data

Supplementary data associated with this article can be found, in the online version, at <http://dx.doi.org/10.1016/j.apcata.2015.05.006>

#### References

- [1] J.J. Bozell, G.R. Petersen, Green Chem. 12 (2010) 539–554.
- [2] P.D. Vaidya, V.V. Mahajani, Ind. Eng. Chem. Res. 42 (2003) 3881–3885.
- [3] H. Li, S. Zhang, H. Luo, Mater. Lett. 58 (2004) 2741–2746.
- [4] C. Xu, L. Zheng, D. Deng, J. Liu, S. Liu, Catal. Commun. 12 (2011) 996–999.
- [5] A. Corma, S. Iborra, A. Velty, Chem. Rev. 107 (2007) 2411–2502.
- [6] K. Yan, G. Wu, T. Lafleur, C. Jarvis, Renew. Sustain. Energy Rev. 38 (2014) 663–676.
- [7] Y. Nakagawa, K. Takada, M. Tamura, K. Tomishige, ACS Catal. 4 (2014) 2718–2726.
- [8] P. Maki-Arvela, J. Hajek, T. Salmi, D.Y. Murzin, Appl. Catal. A: Gen. 292 (2005) 1–49.
- [9] Y. Nakagawa, K. Tomishige, Catal. Commun. 12 (2010) 154–156.
- [10] Y. Nakagawa, H. Nakazawa, H. Watanabe, K. Tomishige, ChemCatChem 4 (2012) 1791–1797.
- [11] N.S. Biradar, A.M. Hengne, S.N. Birajdar, P.S. Niphadkar, P.N. Joshi, C.V. Rode, ACS Sustain. Chem. Eng. 2 (2014) 272–281.
- [12] J. Kijenski, P. Winiarek, T. Paryjczak, A. Lewicki, A. Mikołajska, Appl. Catal. A: Gen. 233 (2002) 171–182.
- [13] K. Yan, J. Liao, X. Wu, X. Xie, RSC Adv. 3 (2013) 3853–3856.
- [14] A.B. Merlo, V. Vetere, J.F. Ruggera, M.L. Casella, Catal. Commun. 10 (2009) 1665–1669.
- [15] I. Wang, W.F. Chang, R.J. Shiao, J.C. Wu, C.S. Chung, J. Catal. 83 (1983) 428–436.
- [16] B.M. Reddy, A. Khan, Catal. Rev. 47 (2005) 257–296.
- [17] C. Lu, Y. Lin, I. Wang, Appl. Catal. A: Gen. 198 (2000) 223–234.
- [18] A.M. Ruppert, T. Paryjczak, Appl. Catal. A: Gen. 320 (2007) 80–90.
- [19] F. Li, T. Lu, B.F. Chen, Z.J. Huang, G.Q. Yuan, Appl. Catal. A: Gen. 478 (2014) 252–258.
- [20] B.S. Akpa, C. D'Agostino, L.F. Gladden, K. Hindle, H. Manyar, J. McGregor, R. Li, M. Neurock, N. Sinha, E.H. Stitt, D. Weber, J.A. Zeitler, D.W. Rooney, J. Catal. 289 (2012) 30–41.
- [21] N.M. Bertero, A.F. Trasarti, C.R. Apesteguia, A.J. Marchi, Appl. Catal. A: Gen. 394 (2011) 228–238.
- [22] C. Reichardt, Chem. Rev. 94 (1994) 2319–2358.
- [23] P.G.N. Mertens, F. Cuyvers, P. Vandezande, X. Ye, F. Verpoort, I.F.J. Vankelecom, D.E. De Vos, Appl. Catal. A: Gen. 325 (2007) 130–139.

- [24] B.M. Reddy, B. Chowdhury, P.G. Smirniotis, *Appl. Catal. A: Gen.* 211 (2001) 19–30.
- [25] B.M. Reddy, P.M. Sreekanth, Y. Yamada, Q. Xu, T. Kobayashi, *Appl. Catal. A: Gen.* 228 (2002) 269–278.
- [26] K. Tanabe, *Catal. Today* 78 (2003) 65–77.
- [27] P. Reyes, D. Salinas, C. Campos, *Quim. Nova* 33 (2010) 777–780.
- [28] K. Fuku, T. Sakano, T. Kamegawa, K. Mori, H. Yamashita, *J. Mater. Chem.* 22 (2012) 16243–16247.
- [29] K. Takanabe, K. Nagaoka, K. Narai, K. Aika, *J. Catal.* 232 (2005) 268–275.
- [30] W. Lin, H. Cheng, J. Ming, Y. Yu, F. Zhao, *J. Catal.* 291 (2012) 149–154.
- [31] S.F. Moya, R.L. Martins, M. Schmal, *Appl. Catal. A: Gen.* 396 (2011) 159–169.
- [32] A. Tanksale, J.N. Beltramini, J.A. Dumesic, G.Q. Lu, *J. Catal.* 258 (2008) 366–377.
- [33] B. Chen, F. Li, Z. Huang, T. Lu, Y. Yuan, G. Yuan, *ChemSusChem* 7 (2014) 202–209.
- [34] M. Komiyama, Y. Ogino, Y. Akai, M. Goto, *J. Chem. Soc., Faraday Trans.* 79 (1983) 1719–1728.
- [35] A.S. Fung, P.A. Tooley, M.J. Kelley, D.C. Koningsberger, B.C. Gates, *J. Phys. Chem.* 95 (1991) 225–234.
- [36] W.E. Pascoe, J.F. Stenberg, *Catalysis in Organic Syntheses*, Academic Press, New York, 1980, pp. 1–3.
- [37] H.S. Broadbent, G.C. Campbell, W.J. Bartley, et al., *J. Org. Chem.* 24 (1959) 1847–1854.
- [38] A.B. Merlo, V. Vetere, J. Ramallo-Loípez, F. Requejo, M. Casella, *React. Kinet. Mech. Catal.* 104 (2011) 467–482.
- [39] P. Claus, A. Bruckner, C. Mohr, H. Hofmeister, *J. Am. Chem. Soc.* 122 (2000) 11430–11439.
- [40] R. Burch, C. Paun, X.M. Cao, P. Crawford, P. Goodrich, C. Hardacre, P. Hu, L. McLaughlin, J. Sá, J.M. Thompson, *J. Catal.* 283 (2011) 89–97.